


Adaptive responses of mature giant chloroplasts in the deep-shade lycopod *Selaginella erythropus* to prolonged light and dark periods

Rabia Ghaffar^{1,3} | Marieluise Weidinger¹ | Barbara Mähner² | Michael Schagerl² | Irene Lichtscheidl¹ 

¹Core Facility Cell Imaging and Ultrastructure Research, University of Vienna, Althanstrasse 14, A-1090 Vienna, Austria

²Department of Limnology and Bio-Oceanography, University of Vienna, Althanstrasse 14, A-1090 Vienna, Austria

³Department of Botany, University of the Punjab, Quaid-e-Azam Campus, Lahore 54590, Pakistan

Correspondence

Irene Lichtscheidl, Core Facility Cell Imaging and Ultrastructure Research, University of Vienna, Althanstrasse 14, A-1090 Vienna, Austria.

Email: irene.lichtscheidl@univie.ac.at

Funding information

Higher Education Commission Pakistan (HEC); Hochschuljubiläumsstiftung der Stadt Wien, Grant/Award Number: H-2115/2010

Abstract

Deep-shade plants have adapted to low-light conditions by varying morphology and physiology of cells and chloroplasts, but it still remains unclear, if prolonged periods of high-light or darkness induce additional modifications in chloroplasts' anatomy and pigment patterns. We studied giant chloroplasts (bizonoplasts) of the deep-shade lycopod *Selaginella erythropus* in epidermal cells of mature fully developed microphylls and subjected them to prolonged darkness and high-light conditions. Chloroplast size and ultrastructure were investigated by light and electron microscopy. Physiological traits were studied by pigment analyses, photosynthetic performance of photosystem II, and formation of reactive oxygen species. Results show that (a) thylakoid patterns and shape of mature bizonoplasts vary in response to light and dark conditions. (b) Prolonged darkness induces transitory formation of prolamellar bodies, which so far have not been described in mature chloroplasts. (c) Photosynthetic activity is linked to structural responses of chloroplasts. (d) Photosystem II is less active in the upper zone of bizonoplasts and more efficient in the grana region. (e) Formation of reactive oxygen species reflects the stress level caused by high-light. We conclude that during prolonged darkness, chlorophyll persists and even increases; prolamellar bodies form de novo in mature chloroplasts; bizonoplasts have spatial heterogeneity of photosynthetic performance.

KEYWORDS

bizonoplast, electron microscopy, etio-chloroplast, micromorphology, PAM, pigments, prolamellar body, rapid light curve, reactive oxygen species, thylakoids

1 | INTRODUCTION

Plants from deep-shade environments such as the understory of dense tropical forests have adapted to low-light by developing distinct morphological traits. Amongst these, optimization of the internal leaf

Abbreviations: bizonoplast, BZ; confocal laser scanning microscopy, CLSM; electron transport rate, ETR; light harvesting complex, LHC; light microscope, LM; photosystem, PS; prolamellar body, PLB; protochlorophyllide, Pchl; pulse amplitude modulated, PAM; rapid light curve, RLC; reactive oxygen species, ROS; transmission electron microscope, TEM

This study is dedicated to the memory of Vassilios Sarafis.

morphology and adaptation of chloroplasts render light exploitation more efficient (Sarafis, 1998). As models for investigating the efficiency of light-entrapping systems, different species of the lycopod *Selaginella* were studied; some of them contain large single chloroplasts in their upper epidermal cells thus exposing an almost continuous layer of chloroplasts to incident light (Haberlandt, 1888, 1905; Jagels, 1970a; Mohling Ma, 1930). The light-harvesting potential as a consequence of the micromorphology of *Selaginella* leaves was described by Waterkeyn and Bienfait (1967) in *S. kraussiana* and by Reshak and Sheue (2012) in *S. erythropus*; the chloroplast structure was related to light exploitation.

This is an open access article under the terms of the Creative Commons Attribution License, which permits use, distribution and reproduction in any medium, provided the original work is properly cited.

© 2018 The Authors Plant, Cell & Environment Published by John Wiley & Sons Ltd

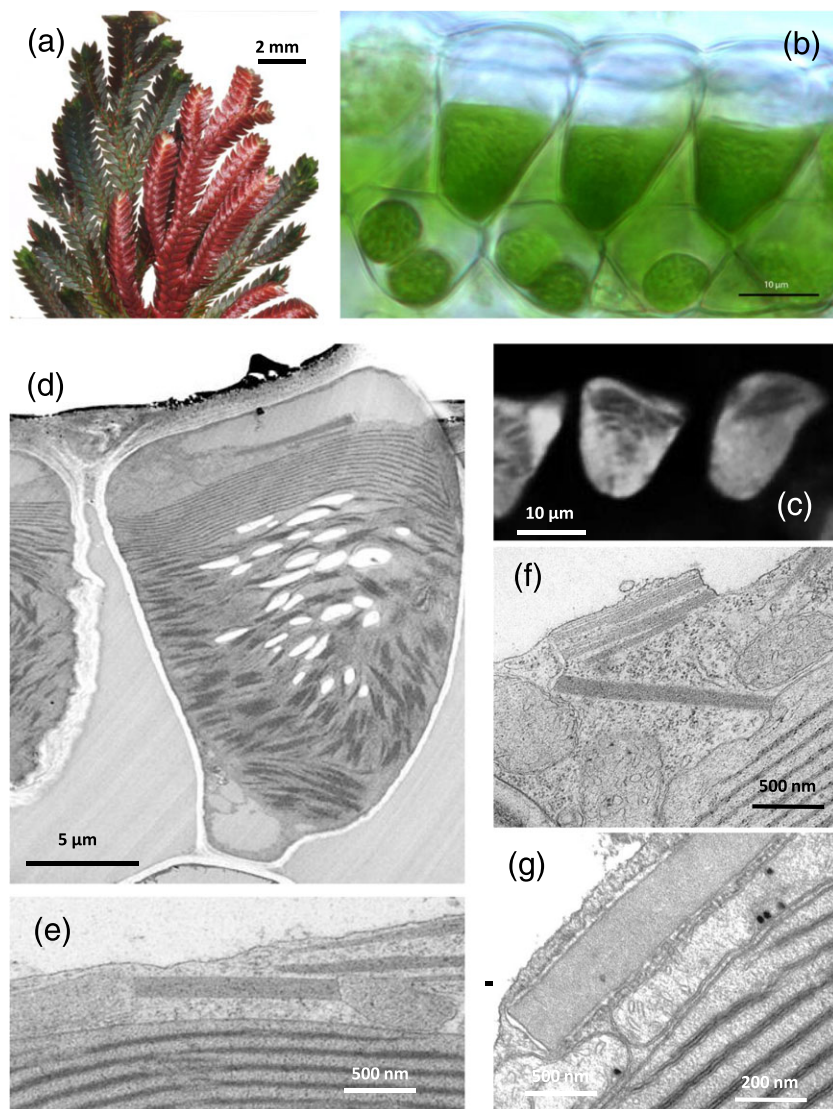


FIGURE 1 *S. erythropus*: Microphylls of plants from control shade conditions. (a) Part of the shoot system with the arrangement of dimorphic microphylls; they lie flat and open along the stem axis with dark green ventral and red dorsal surfaces. (b) Bright-field image of a cross-section through a microphyll: Upper epidermal bizonoplasts fill the whole conical part of the cells, whereas the lower mesophyll cells have roundish chloroplasts. A slight partition between the two regions in the bizonoplasts is also visible. Grana appear as dark shadowed flecks in the lower part and an upper agranal region is visible as a thin, clear zone. (c) Autofluorescent bizonoplasts in confocal laser scanning microscopy: The upper and lower regions can be distinguished by different fluorescence intensities; non-fluorescent minute spots indicate the position of starch grains scattered between these two regions, dish-like depressions are visible in the middle and right bizonoplasts at their top. (d) Transmission electron microscope micrographs showing the cover of parallel thylakoids on top of the granal region of a bizonoplast, with the starch in the center, and the cytoplasm around. (e–g) The upper cytoplasmic region topping the bizonoplasts contains peroxisomes which are in close contact with proteinaceous paracrystalline rods and partly surrounded by endoplasmic reticulum

Selaginella erythropus is a creeping or ascendant plant with simple, scale-like leaves called microphylls on branching stems from which also roots arise. Microphylls have a green upper and reddish lower surface and are arranged in rows along the stems; microphylls in the ventral rows are larger compared with those of dorsal rows (Figure 1a). The microphylls have one single vein that is part of the vascular system. In the mid-vein region, both types of microphylls are six cell layers thick and reduce to two layers (upper and lower epidermis) towards the margins. In the upper epidermis of both types of microphylls, cells are funnel-shaped, with one characteristic giant chloroplast. Its structural and physiological reactions and its sensitivity to light have been described in detail by Jagels (1970a, 1970b). It was hypothesized that the special shape of the giant chloroplasts increases efficiency of light-harvesting. A similar conclusion was made by Héban and Lee (1984), when they described the iridescence of some *Selaginella* species as a physical effect of light absorption regarding wavelengths above 450 nm, especially also in the far red region. Sheue et al. (2007) described the ultrastructure of the giant chloroplasts in *S. erythropus* and detected two different kinds of thylakoid arrangements: (a) a lower zone where thylakoids are organized in grana and stroma thylakoids similar to the structure of typical chloroplasts of higher plants and (b)

an upper zone that forms a lens-shaped cover of several stacks of three elongated thylakoids. They named it therefore "bizonoplast" (BZ).

Plants adapted to deep-shade have to cope also with specks of intense light where the sun breaks through bare areas of the canopy. Sudden exposure to excess light leads to the formation of reactive oxygen species (ROS), which causes oxidative damage to proteins, DNA, and lipids and leads to irreversible damage and necrosis (Halliwell, 2006, and reviews by Suzuki, Koussevitzky, Mittler, & Miller, 2011, Sharma, Jha, Dubey, & Pessarakli, 2012). Plants therefore developed photoprotective measures against excess light such as accessory photosynthetic pigments and adaptation of leaf and cell morphology. Recently, the development of young BZs in *S. erythropus* grown under high-light conditions was investigated and their physiological response was described (Sheue et al., 2015). The response of epidermal BZs and mesophyll chloroplasts in mature cells however remained unclear, and also, a possible response of such mature chloroplasts to prolonged darkness is still unknown. Moreover, possible reactions of *S. erythropus* grown at low-light conditions comparable with the natural environments and suddenly exposed to high irradiances remain unclear to date. From an ecological perspective, these questions are fundamental for survival of the plants, as prolonged darkness is a frequent event for small deep-shade

plants such as *Selaginella*, which are easily covered by organic material (e.g., fallen leaves and twigs). Also, an abrupt and prolonged rise in light caused, for example, by broken canopy occurs frequently in nature.

To bridge this gap of knowledge, we studied reactions of fully developed BZs in mature leaves of *Selaginella erythropus* towards changed light conditions from prolonged darkness to high-light. We relate structural changes of the chloroplasts to changes of the photosynthetic performance and pigment patterns, and we discuss changes of chlorophyll and the formation of ROS as indicators for stress.

2 | MATERIALS AND METHODS

2.1 | Growth conditions and sampling

Selaginella erythropus (red spike-moss) was sampled from the Singapore Botanic Gardens by courtesy of late Prof. V. Sarafis (Queensland University, Australia). Plants were cultivated in the greenhouse of the University of Vienna at a 12-hr light-and-dark cycle in weak light corresponding to its natural environment ($15 \mu\text{mol photons PAR m}^{-2} \text{ s}^{-1}$), which assured optimum growth conditions. These specimens were regarded as controls. Responses to prolonged darkness were tested in plants grown under the same conditions (humidity, temperature), but in darkness for 24, 48, 72, and 96 hr. The reactions to prolonged high-light were set according to pilot tests, which showed that *Selaginella* as a deep-shade plant achieves light saturation at around $50\text{--}60 \mu\text{mol photons m}^{-2} \text{ s}^{-1}$. From this test, we set high-light conditions at $75 \mu\text{mol photons PAR m}^{-2} \text{ s}^{-1}$ for corresponding time intervals, which were induced by illuminating plants with fluorescence tubes.

In order to ensure comparable developmental stages of the cells, mature microphylls were sampled at a distance of 10 mm from the tip of the branches (fronds). All preparatory steps were carried out under dim light.

2.2 | Light and electron microscopy

The morphology of microphylls was investigated with bright field and wide field fluorescence light microscopy (LM; Olympus BX41). Chloroplast volumes were calculated with the programme digital image analysis in microbial ecology (Daims, Lucker, & Wagner, 2006). Additional information of the three-dimensional structure of the chloroplasts and their surrounding cytoplasm was obtained by means of a confocal laser scanning microscope (Leica SP5). Chloroplasts were detected by their autofluorescence at 680 and 730 nm, mitochondria gave fluorescence with Rhodamine 123 (Sigma, $1 \mu\text{M}$ in water). ROS were labelled with the fluorescence dye 2',7'-dichlorofluorescein diacetate (H2DCF, Sigma, $5 \mu\text{M}$ in water). Laser lines of a white light laser and detectors were set to avoid cross-fluorescence. For ROS detection, the baseline fluorescence intensity of the cytoplasm of control shade cells was determined. Increase of fluorescence by ROS formation upon illumination was estimated from increased detector signals (three different plants for each treatment, 10 microphylls each). Dead cells served as negative controls.

For transmission electron microscopy (TEM) studies, thick cell walls and cuticle needed some modifications of the standard protocol. After fixing leaves in 2.5% glutaraldehyde in 0.1 M sodium-cacodylate buffer for 3 hr, they were rinsed with 0.05 M sodium-cacodylate buffer three times for 10 min each. Postfixation with 1% osmium tetroxide

overnight was followed by three short rinsing steps in 0.05 M buffer. The tissue was dehydrated in 100% dimethoxypropane for 10 min followed by 100% acetone 3×5 min each. Infiltration of resin (Agar 100 Low Viscosity Resin) was carried out as follows: mixture of acetonitrile:resin 3:1 for 3 hr; 1:1 mixture of acetonitrile:resin overnight; 100% resin 4–5 hr; evacuated and left overnight in 100% resin. On the following day, samples were transferred to fresh 100% resin and placed for 10 min at 40 °C, evacuated, and placed again for 10 min at 40 °C; finally, the leaves were embedded in resin at 40 °C for 4 hr and left overnight at 60 °C.

Semithin sections for overview in the LM were stained with toluidine blue. Ultrathin sections were prepared, stained with uranyl acetate and lead citrate, and observed at a TEM Zeiss Libra 120. We observed in total 60 sections per microphyll; each section was screened for the plastids from upper and lower epidermis as well as for mesophyll cells.

2.3 | Pulse amplitude modulated (PAM) fluorescence measurements and high performance liquid chromatography (HPLC) pigment analyses

Seven *Selaginella* plants of every light treatment were chosen for obtaining maximum dark fluorescence yields of photosystem II (PSII). First, fresh mass of specimens was obtained. After 20 min predarkening, measurements were taken at five different spots of each branch on the upper leaf side (Diving PAM, Walz company). The maximum fluorescence dark yield (F_v/F_m) of PSII is defined as $F_v/F_m = (F_m - F_0)/F_m$ (Maxwell & Johnson, 2000) and provides information about the overall photosynthetic performance; a reduced F_v/F_m indicates different types of plant stress. F_m represents the maximum dark fluorescence after a strong flash of light (all PSII reduced), F_0 the minimum (all PSII oxidized), and F_v the variable fluorescence. For additional information about the actual light acclimation state of plants, rapid light curves (RLCs) were measured at five branches per light treatment for the samples of 48 hr light, 48 hr dark, 96 hr light, 96 hr dark and control (three measurements on different spots of each branch were averaged; predarkening 5 min). Relative electron transport rates (ETR) were calculated as $\text{ETR} = \text{PAR} \times 0.5 \times F_v'/F_m'$, where PAR is incoming photosynthetically active radiation, F_v' = variable fluorescence at ambient light, and F_m' = maximum fluorescence at ambient light (Schreiber, Klughammer, & Kolbowski, 2012). To get insight into the spatial activity of PSII located in BZs, the intensity of fluorescence yields was visualized by means of an imaging PAM fluorescence device (Imaging PAM M-Series, Microscopy version, Walz company).

Immediately after PAM-measurements, plants were shock-frozen with liquid nitrogen and stored at -80°C for further pigment analyses. For pigment extraction, plants were cut into small pieces; 3 ml of 90% acetone were added to each sample, homogenized with an ultrasonic probe, and stored for 12 hr in the dark at 4 °C. The samples were then centrifuged and the supernatant taken for analysis of lipophilic pigments (HPLC La Chrome Elite Hitachi equipped with diode array detector-L-2455 and L-2485 fluorescence detector; column Merck-Superspher 250/4 RP-18; precolumn: Merck-Lichrospher RP-8 endcapped). A ternary low-pressure gradient was applied for separation of pigments (Wright et al., 1991), detection was done at 440 nm. Pigment identification was performed by co-chromatography

of standards (DHI LAB company) and comparison of specific absorption maxima (Jeffrey, Mantoura, & Wright, 1997; Roy, Llewellyn, Egeland, & Johnsen, 2011). For protochlorophyllide (Pchl_{id}), cress seedlings were grown for 7 days in the dark. The same extraction procedure and HPLC analysis were applied as for *Selaginella*. Absorption spectra of Pchl_{id} were identified after Helfrich, Ross, King, Turner, and Larkum (1999) and Reinbothe, Pollmann, and Reinbothe (2003).

Pigment contents and dark yields were analysed with Sigmaplot 12.5 (Systat Software, San Jose, CA, USA) by using the ANOVA with level of significance p values = .05 (Normality Test [Shapiro–Wilk] and Equal Variance Test were calculated before). For pairwise multiple comparisons of controls and treatments, Holm–Sidak tests were applied with overall significance level p = .05. Sigma Plot 12.5 was used for visualizing the data in graphs.

3 | RESULTS

3.1 | Morphology of microphylls and their cells

BZs are located in the upper epidermis of microphylls; they fill the lower, narrow portion of funnel-shaped epidermal cells almost completely (Figure 1b). TEM micrographs reveal a thin layer of cytoplasm in their lateral surrounding (Figure 1d). The upper part of the cells contains the major portion of the cytoplasm including—among the usual organelles—a large vacuole and a conspicuous amount of paracrystalline rods (Figures 1e–g). These rods are of homogeneous but grainy appearance, like other proteinaceous inclusions in plants. They either lie free within the cytoplasm or are in direct contact to peroxisomes and endoplasmic reticulum (ER).

In a few cases, the endoplasmic reticulum even seems to surround the paracrystalline rod (Figure 1g). As the presence of these rods is obviously not linked to light and dark regimes, their cytological role was not further investigated in this context.

In contrast to the upper epidermis, mesophyll cells contain two to four spherical to ovoid chloroplasts with uniform arrangement of granal and agranal thylakoids (Figure 1b). The same ultrastructure is found in the chloroplasts of the lower (abaxial) epidermis; these chloroplasts are, however, smaller and interconnected to chains (not shown).

Size and form of the BZs were investigated under different light intensities and their microanatomy was revealed from autofluorescence of the chlorophyll in fluorescence microscopy (Figure 1c) and from ultrastructural details of TEM micrographs.

3.2 | Morphological aspects of BZs from control shade conditions

BZs fill up to 65% of the cell volume and have a mean diameter of 10.52 μm in comparison with the mean cell diameter of 16.82 μm . Using confocal laser scanning microscopy (CLSM) image data and applying the quantification method “digital image analysis in microbial ecology”, DAIME, the mean volume of BZs was calculated to be $483 \pm 88 \mu\text{m}^3$. The cone-shaped BZ fills the lower part of the epidermal cell with its tapering end; its upper flat broader part faces the incident light. Originally, BZs were described as cups (Sheue et al., 2007). Also, in our investigations, CLSM images show strong fluorescence of plastids with dish-like cavities or depressions

(Figure 1c). Comparison of CLSM and TEM images reveals that the cavities correspond to the lower part of BZs containing the common arrangement of thylakoids, that is, grana stacks and stroma lamellae (Figures 1c,d and 2b). The layer on top of these cups has weak fluorescence that becomes visible by careful tuning of the CLSM detectors (Figure 1c). It corresponds to the long extended parallel thylakoid stacks (three to four thylakoids, 44 nm per stack; Figures 1d and 2a) covering the whole upper surface of the BZ as seen by TEM. Thylakoids may be arranged in different directions but are mainly orientated in parallel to the upper cell wall. The lower zone of BZs contains stroma and grana thylakoids and is interspersed by starch grains that occur mainly in the central region. At first sight, darkly stained grana stacks appear as individual entities and resemble the membrane distribution of chloroplasts in higher plants (Figure 1d).

Closer inspection of TEM images reveals, however, that almost all grana thylakoids are connected to stroma thylakoids that have less contrast and are slightly inflated. Stroma and grana thylakoids hence represent a continuum throughout the lower zone of the BZ (Figures 1d and 2b), they form extended sheets covering large areas similar to thylakoids in the upper zone. In the regions of grana stacks, they are appressed to each other much more densely, and the accumulated pigments, enzymes, and apoproteins forming the PSI and PSII and light harvesting complexes I and II (LHCI and LHCII; stained with uranyl-acetate and lead citrate) cause dark staining (Figure 2c,d).

3.3 | Morphological aspects of BZs from dark-treated microphylls

BZs turn into a spherical shape and their volume gradually increases to an average volume of 818 μm^3 . The clear differentiation between upper and lower zone is preserved throughout this period; there are, however, structural rearrangements visible within each zone (Figure 3a).

In the upper zone, the extended thylakoids become more distinctly stained already after 24 and 48 hr of darkness, and also, the interspace between these thylakoids has depositions of dark staining that become more pronounced (Figure 3a,c). The delimiting thylakoids of the stacks (two to four thylakoids) widen so that their lumen becomes clearly visible. These changes are, however, reversible; after 72 and 96 hr darkness (Figure 3d), no difference is visible in comparison with the controls.

In the lower zone, grana stacks increase in height from 268 nm (control, Figure 1d) to 385 nm (Figure 3b,d) and in the average number of thylakoids per stack from 15 (control) to 21. Small vesicles confine the inner envelope of the BZs (Figure 3b). Stroma lamellae continue to fill the space between the grana stacks; they are undulating and have a beaded and swollen appearance (Figure 3d).

Starch grains peak in number during the first 24 hr. The grains are scattered throughout the lower part of the BZs (Figure 3a), and even after 96 hr darkness, a few small starch grains still remain in the central region between upper and lower zone (Figure 3d).

3.4 | De novo formation of prolamellar bodies in mature BZs after a period of 48 hr darkness

An unusual, so far unobserved feature of the BZs is the appearance of crystalline structures known as prolamellar bodies (PLBs) within the

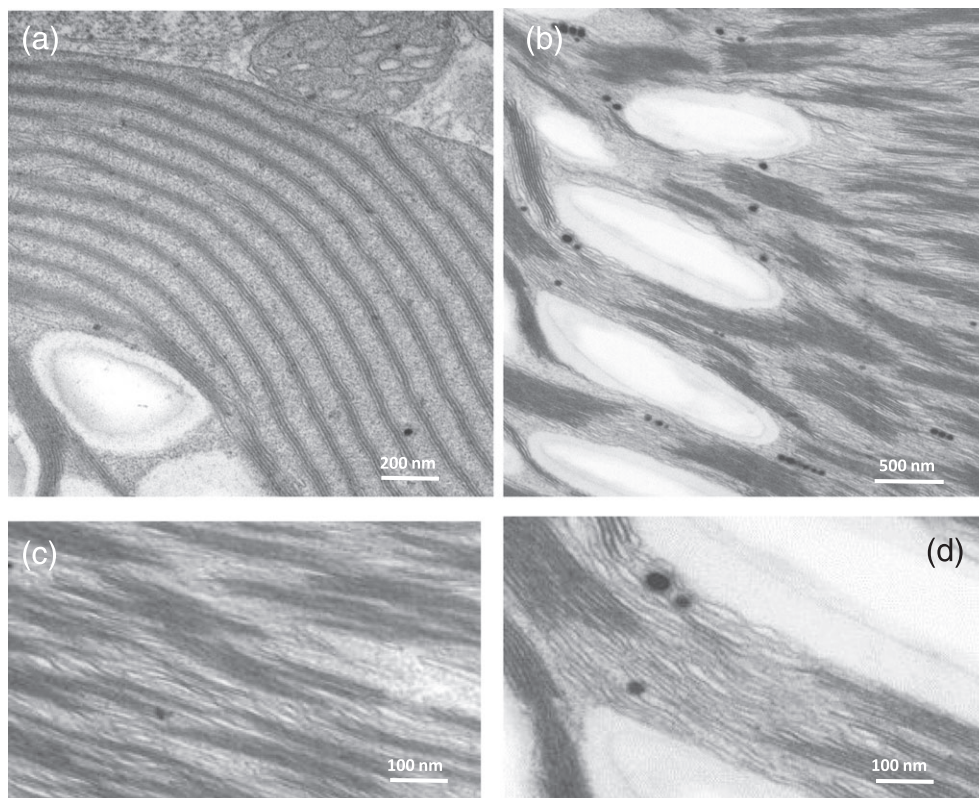


FIGURE 2 Transmission electron microscope micrographs of bizonoplasts from shade conditions illustrating the thylakoid arrangement in the upper and lower zone. (a) Upper agranal zone of bizonoplast with parallel stacks of three to four thylakoids. (b) Lower granal zone of bizonoplast with coined grana stacks; translucent starch grains and circular electron dense plastoglobuli are scattered in granal region. (c,d) Granal thylakoids connect to the stroma lamellae thus forming a continuum

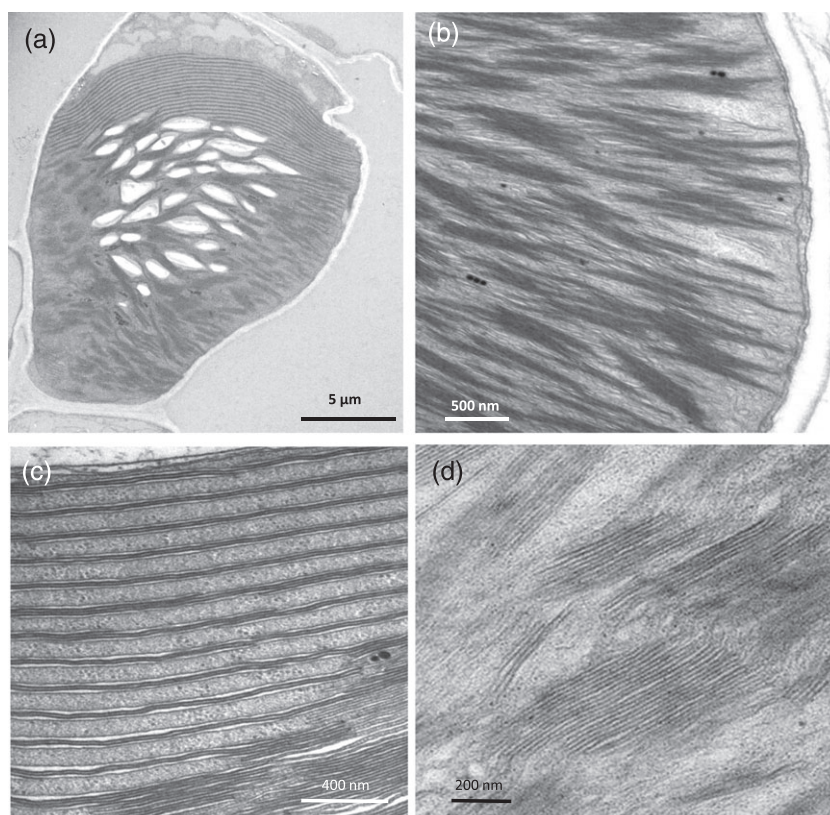


FIGURE 3 Transmission electron microscope micrographs of bizonoplasts from dark treatment for variable durations showing structural variations. (a) Bizonoplast after 24 hr darkness still carries the two zones and starch grains. (b) The lower granal zone of bizonoplast again from 24 hr darkness shows the small vesicles confined to the inner envelope. (c) The upper agranal zone of BZ after 48 hr darkness shows widely spaced delimiting thylakoids and more electron dense material between the inter-thylakoidal space in each stack. (d) A portion from the bizonoplast in 96 hr darkness that shows higher grana stacks with more spacing between grana thylakoids; stroma lamellae are undulating and have a beaded and swollen appearance

dense network of stroma thylakoids. They become visible in ultrathin TEM sections after a dark period of 48 hr but disappear at prolonged darkness of 72 and 96 hr. We counted up to 10 PLBs per BZ in one ultrathin section; diameters of PLBs range between 200 and 500 nm in cross-section with an average diameter of 328 nm (Figure 4a).

Each PLB is a compound structure of repeated unit membranes forming a regular lattice. Varying numbers of unit tubules aggregate in different geometric forms resulting in different PLB configurations. In the two-dimensional micrographs of consecutive ultrathin sections, we observed basically three different PLB conformations: circular PLBs

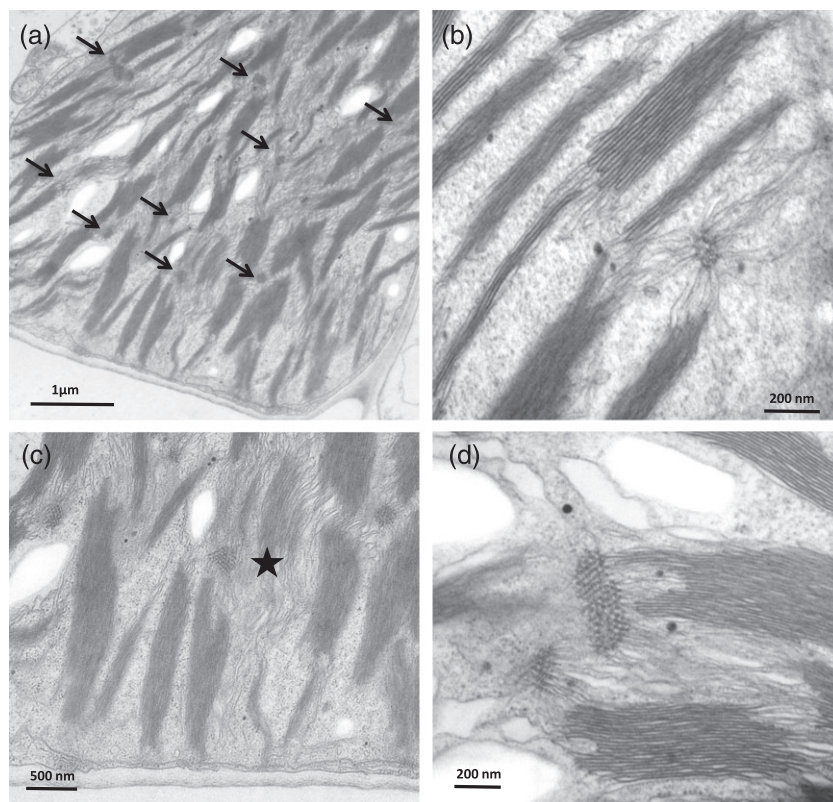


FIGURE 4 Transmission electron microscope micrographs of bizonoplasts from 48 hr dark period illustrating prolamellar bodies within the established thylakoid network. Stroma and grana thylakoids remain. (a) Prolamellar bodies appear between grana stacks in the lower zone. Arrows point at individual prolamellar bodies that are connected to their neighbouring grana stacks. (b) Tubular units of the crystalline body form circular arrangements. (c) A triangular prolamellar body (asterisk). (d) Rectangular prolamellar body

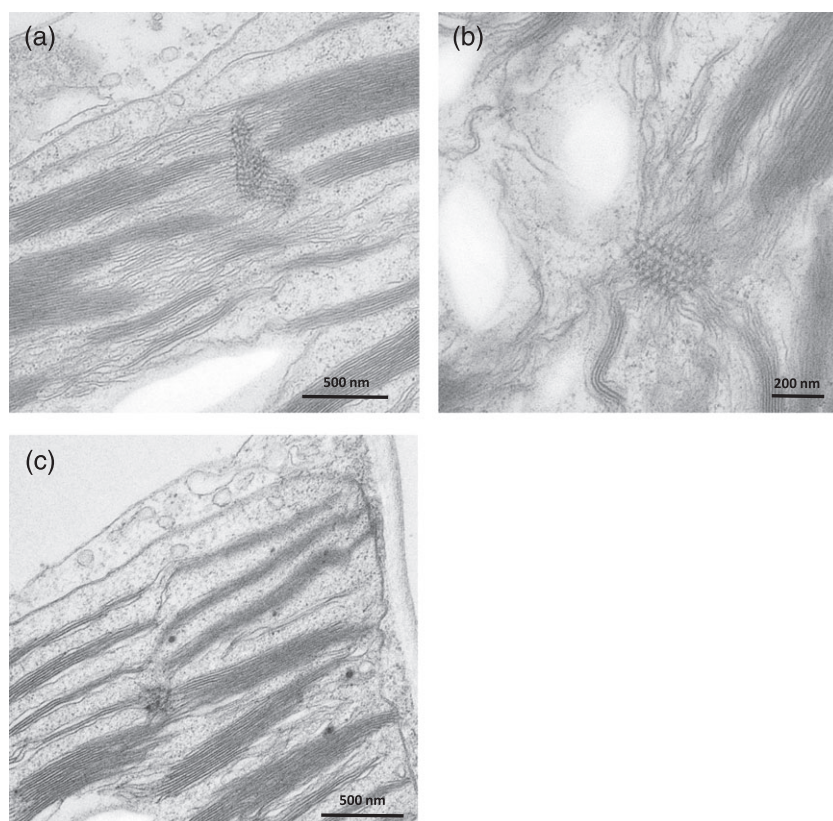


FIGURE 5 Transmission electron microscope micrographs illustrating the prolamellar body connections with grana thylakoids. (a) A group of three interconnected prolamellar bodies; emerging stroma lamellae from prolamellar bodies connect to the grana thylakoids. (b) Tubular units are clearly visible in the prolamellar body, each margin tubule of the prolamellar body connects to a stroma or grana thylakoid. (c) Stroma thylakoids from prolamellar bodies reach into the upper agranal zone and connect to elongated parallel thylakoids

(Figure 4b) where tubular units are evenly distributed, triangular PLBs (Figure 4c) showing one decreasing unit in each successive layer of their framework, and extended PLBs (Figure 4d) with rectangular alignment of tubular units.

PLBs are embedded in the stroma and interconnect to grana stacks and to neighbouring PLBs via stroma thylakoids; from each margin tubule of a PLB, a stroma thylakoid emerges and connects to a specific sheet of the granal stack. The larger the PLB, the more stroma lamellae emerge from it, and the more grana thylakoids can be reached by them (Figure 5a,b). We occasionally observed that stroma thylakoids from PLBs radiate also into the upper zone of BZs and connect to its long parallel thylakoids (Figure 5c). In these

cases, however, they still remain connected also to grana stacks of the lower zone.

3.5 | De novo formation of PLBs in mesophyll cells

Chloroplasts from mesophyll cells resemble typical plastids of shade plants; they are big and contain abundant grana stacks and stroma thylakoids, but the upper zone typical for BZs is missing (Figure 6a). The mesophyll chloroplasts are 5–6 μm in diameter, about half the size of BZs (12 μm) but still much larger than chloroplasts of the lower epidermis (2.5 μm). Starch granules are present along with ribosomes and few plastoglobules. After 48 hr darkness, PLBs are also found in

FIGURE 6 Transmission electron microscope micrographs of mesophyll chloroplasts from 48 hr dark treated microphylls show prolamellar bodies with similar ultrastructure as in bizonoplasts. (a) Intergranal prolamellar bodies established within free stroma space and link to grana thylakoids. (b) Two adjacent prolamellar bodies connect through stroma thylakoids among each other and to the adjacent grana stacks

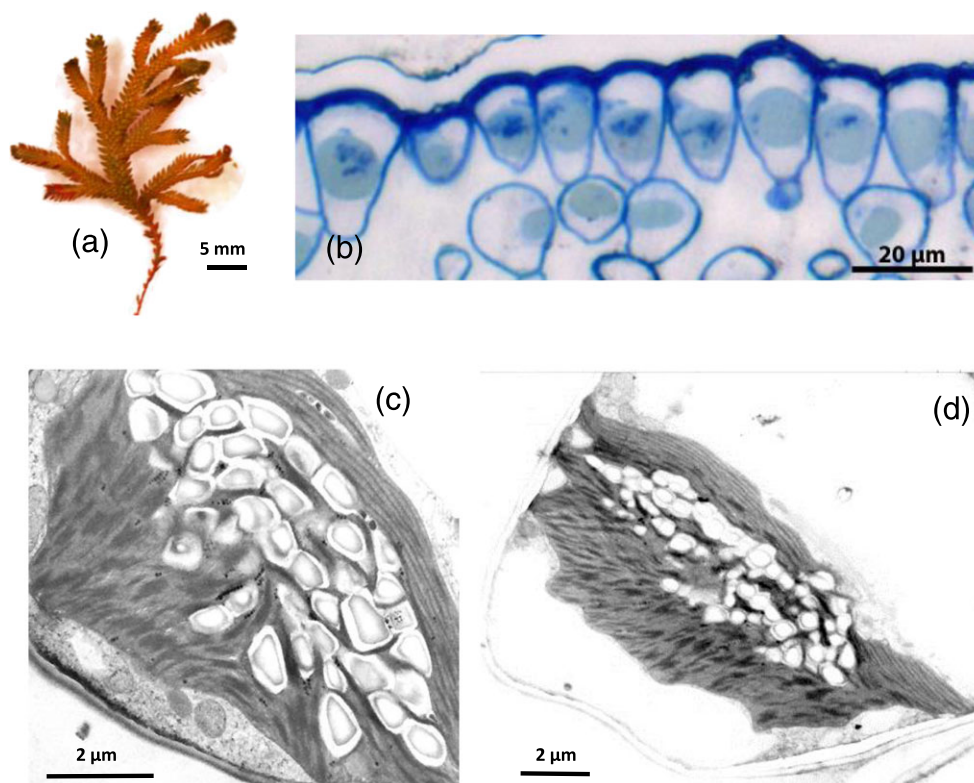
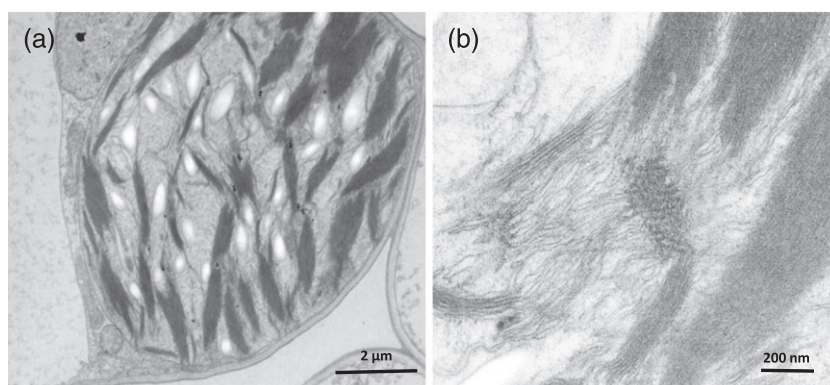


FIGURE 7 *S. erythropus* after 48 hr in high-light intensity. (a) A shoot with microphylls more widely spaced and greenish yellow in colour. (b) Semithin section from these microphylls shows detachment of bizonoplasts from the cell walls and their upward movement. (c,d) Transmission electron microscope micrographs from the microphylls of the same treatment show distorted forms of bizonoplasts; however, zonation into upper and lower zone is maintained. Starch grains accumulate

mesophyll chloroplasts with structures similar to those in BZs. Tubules radiating from the periphery are again continuous with stroma lamellae (Figure 6b).

3.6 | Bizonoplasts in strong light

High-light conditions ($75 \mu\text{mol photons PAR m}^{-2} \text{ s}^{-1}$) causes growth inhibition and bleaching of the microphylls within 1 week (Figure 7a). BZs almost double their volume to $800\text{--}950 \mu\text{m}^3$ during the first 2 days (not shown) and then shrink again to their original size. They lose their conical form, develop infoldings, and retract from the cell membrane. They become stuffed with starch grains, which increase in both number and size and fill large parts of the centre between upper and lower zones (Figure 7b–d). The upper zone of parallel thylakoids decreases in height (439 nm) but remains throughout the light treatment. Also, grana stacks of the lower zone reduce their number of thylakoids, their height (266 nm), and their diameter (641 nm). Orientation of grana stacks varies from perpendicular to parallel along the short axis of BZs.

When microphylls start to bleach, BZs apparently disintegrate into two to four parts. Light microscopical results indicate independent and separated fragments (Figure 8a), but TEM data revealed that the small entities are still connected by extensions of the chloroplast envelope similar to stromules (Figure 8b); they hence represent lobes of the original BZs. Each lobe is about $213 \mu\text{m}^3$ in volume on average and is positioned along the anticlinal cell walls. Some lobes carry the parallel layers of thylakoids from the upper zone and only few rudimentary grana with maximum of three to four thylakoids per stack, some lobes contain only grana thylakoids from the lower zone (Figure 8c). Number of plastoglobules increases; they form chains but are also scattered in groups among the grana stacks in the stroma. Stroma lamellae decrease with increasing illumination time (Figure 8d).

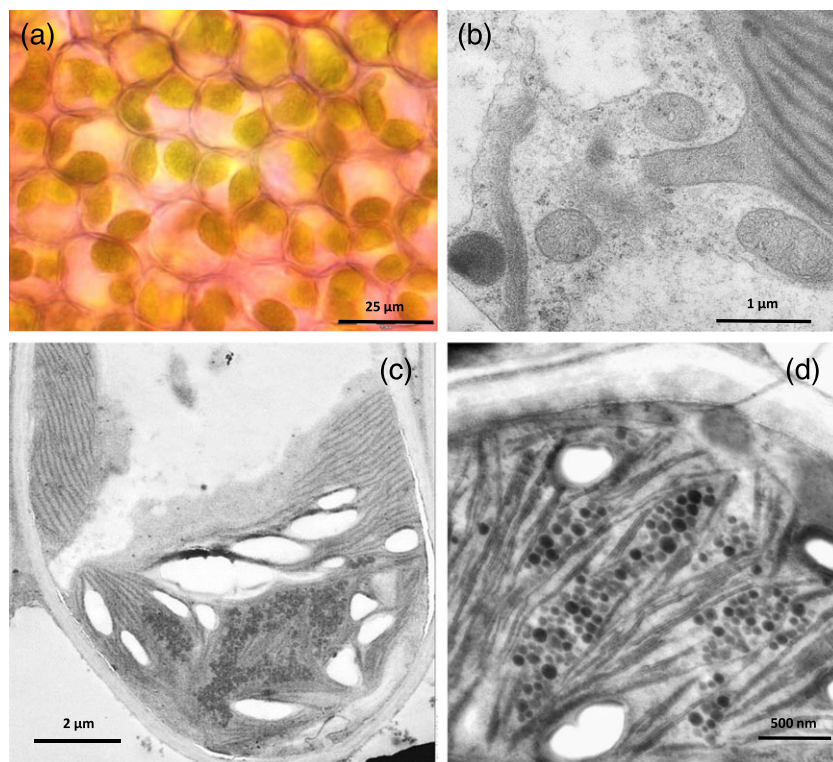


FIGURE 8 Bizonoplasts disintegrate into lobes after prolonged illumination of 96 hr. (a) Bright-field image of the epidermal cells shows fractionation of the bizonoplast into two or more lobes. (b) Transmission electron microscope micrograph reveals that chloroplast fractions are interconnected by tubular protrusions similar to stromules; elongating plastid envelope contains plastid stroma but no thylakoids. (c) The parallel arrangement of thylakoids in the upper zone is maintained, although split among the lobes. (d) The thylakoids of the granal zone reduce in number and plastoglobuli develop

3.7 | Physiological responses to prolonged light/darkness

Plants react to different light treatments with changes in pigments concentrations, overall photosynthetic performance, and increased release of ROS.

3.7.1 | Pigment patterns

The photosynthetic pigments resemble those of higher plants with chlorophylls-a and -b, neoxanthin, violaxanthin, lutein, and β -carotene

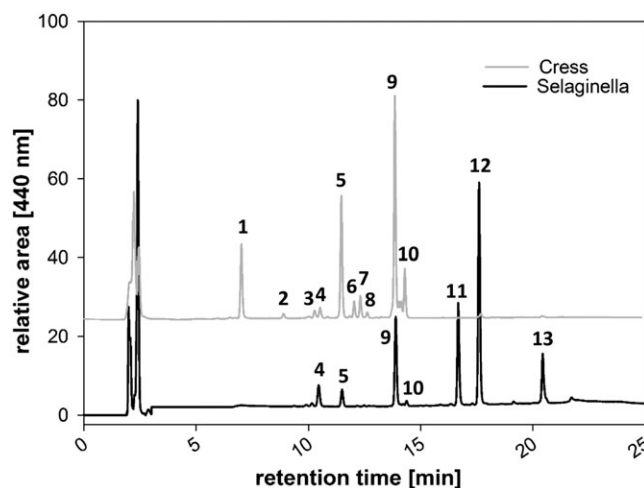


FIGURE 9 Chromatograms of etiolated cress seedlings (grey line) and *Selaginella* cultivated 48 hr in darkness (black line) with prolamellar bodies. 1 = protochlorophyllide, 2 = all-trans-Neoxanthin, 4 = cis-Neoxanthin, 5 = Violaxanthin, 8 = Antheraxanthin, 9 = Lutein, 11 = chlorophyll-b, 12 = chlorophyll-a, 13 = β -carotene, 3,6,7,10 = unknown xanthophylls

as main components (Figure 9). Pchl_{ide} is sometimes found in traces in mature *Selaginella* (quantification not possible); etiolated seedlings (controls) show high amounts of this chlorophyll precursor (Figure 9). For chlorophylls-a, -b, and lutein per unit biomass, a significant decrease is recognized after 48 hr darkness, which is followed by a pronounced increase (Figure 10). Based on chlorophyll-a, none of the pigments show significant changes after 48 hr darkness, but prolonged darkness of 96 hr results in a pronounced increase of both chlorophylls, which is stronger than that of the remaining pigments. With the exception of β -carotene, high-light treatment causes a significant drop in pigment concentrations already after 48 hr. The bleaching is also visible with the naked eye.

3.8 | Photosynthetic performance of plants

F_v/F_m of controls and plants exposed to prolonged darkness are in the same range between 0.71 and 0.74 (median; Figure 11) but decrease significantly during prolonged high-light treatments (F_v/F_m after 96 hr = 0.56). RLCs of controls display a shape characteristic of shade plants with steep initial slopes (Figure 12). Moreover, the controls show the highest ETRs compared with all other treatments. Both 48 h treatments react in a very similar manner with almost identical initial slopes and slightly decreased maximum ETRs; 96 h treatments

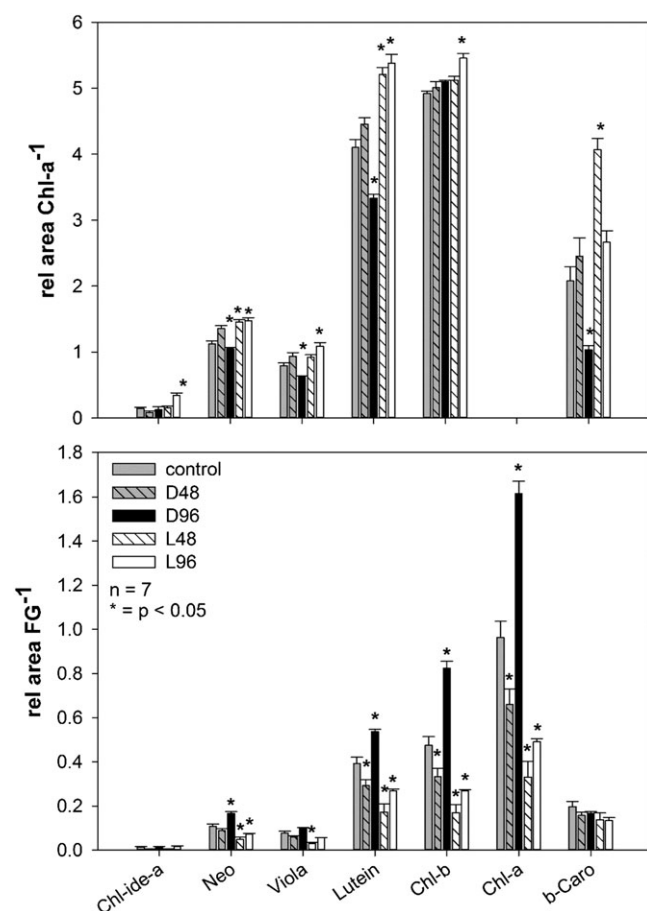


FIGURE 10 Major photosynthetic pigments of *Selaginella erythropus* (relative absorption units per unit chlorophyll-a (top) and fresh mass (bottom)). Chl-ide-a = chlorophyllide-a, neo = Neoxanthin, Viola = violaxanthin, Chl-b = chlorophyll-b, Chl-a = chlorophyll-a, b-Caro = β -carotene; * = significant difference to control, $p < .05$

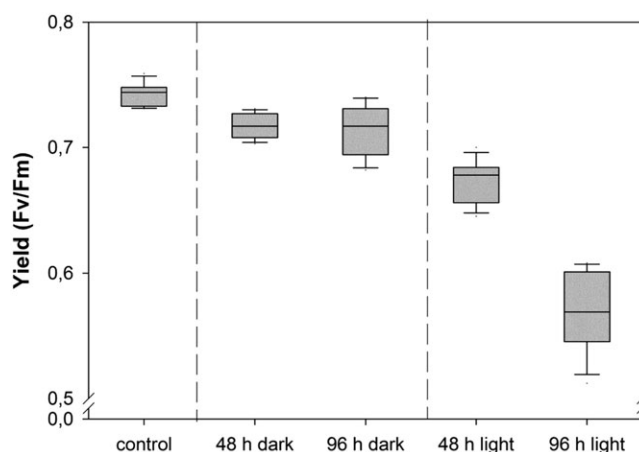


FIGURE 11 Fluorescence dark yields (F_v/F_m) of different treatments. Median boxes 5-25-50-75-95% percentiles. n per treatment = 7

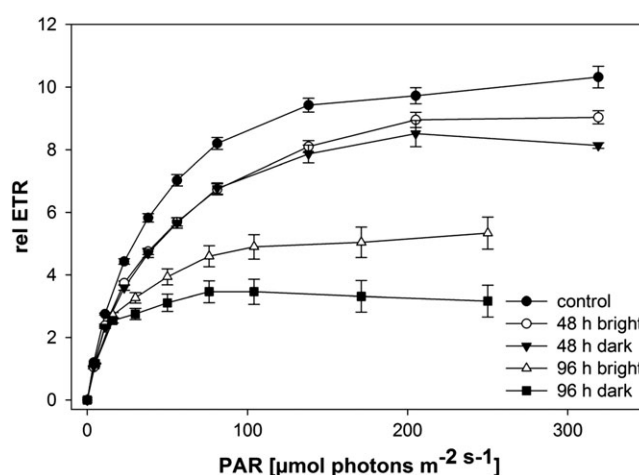


FIGURE 12 Rapid light curves of different treatments. Rel ETR = relative electron transport rate. n per treatment = 7. Symbols are means; error bars are standard deviations

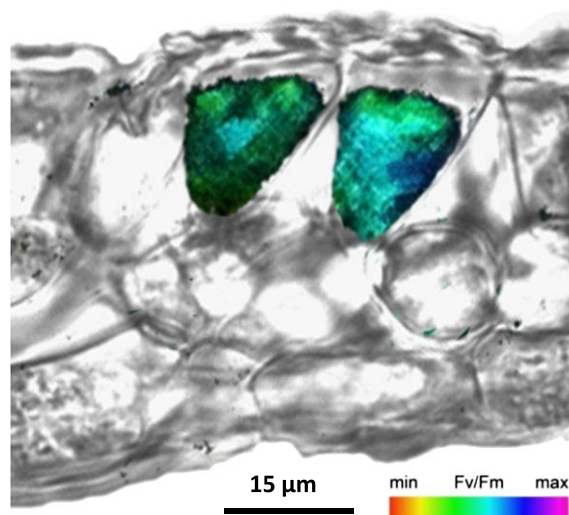


FIGURE 13 Cross-section of a microphyll with two intact bizonoplasts. The colour bar indicates fluorescence yields under weak illumination. Upper zones with long extended parallel thylakoid stacks show weaker photosynthetic activity compared with lower zones with typical grana stacks and stroma lamellae

display a strong drop in maximum ETRs with 96 hr dark-exposed plants showing the lowest values.

3.9 | Photosynthetic activity on a cellular level

Thin sections of microphylls provided some intact cells with lateral views of BZs (Figure 13). Upper parts of BZs facing the incoming light (thylakoids mostly arranged in parallels with no grana stacks) show decreased fluorescence yields compared with regions with distinct grana stacks. Compared with controls, PAM-fluorescence images of intact plants indicate slightly decreased F_v/F_m of plants exposed to 48 hr darkness (Figure 14). Specimens exposed to 48 hr high-light

show a significant decrease of F_v/F_m especially in regions facing the incoming light (Figure 14).

3.10 | Reactive oxygen species

Staining the leaves with H2DCF-DA yields green fluorescence of ROS and allows localizing them in various subcellular compartments. In the controls, fluorescence is emitted from spherical or rod-shaped organelles; some were identified as mitochondria by co-labelling with rhodamine 123; others did not react with rhodamine 123 and were considered as peroxisomes (also proved by means of TEM). Fluorescence is also emitted within nucleus and BZs. The cytoplasm around the giant BZs remains dark (Figure 15a).

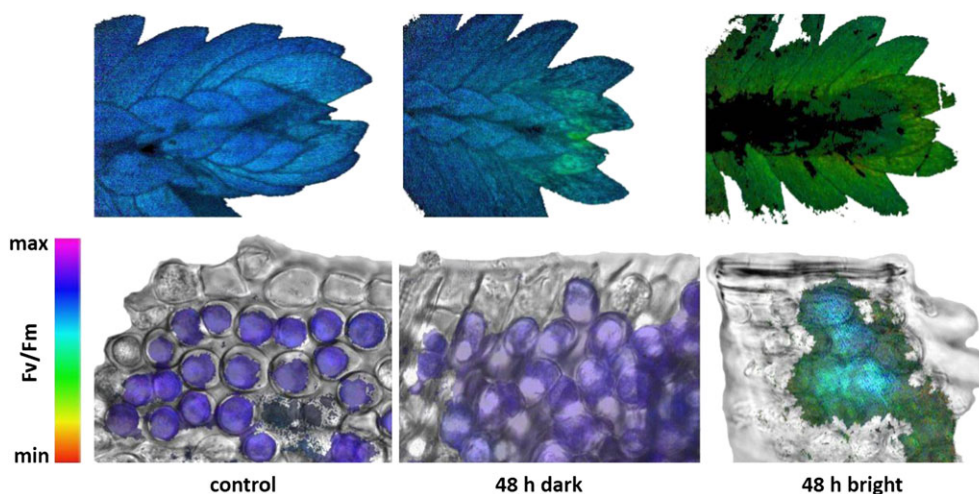


FIGURE 14 Maximum dark fluorescence yields (F_v/F_m) of microphylls after treatments. The colour bar indicates fluorescence yields on a relative scale. The upper photos show tips of branches, the lower photos corresponding microphylls with intact cells. Compared with the control and the 48 hr dark treatment, 48 hr illumination with high-light causes severe photodamage

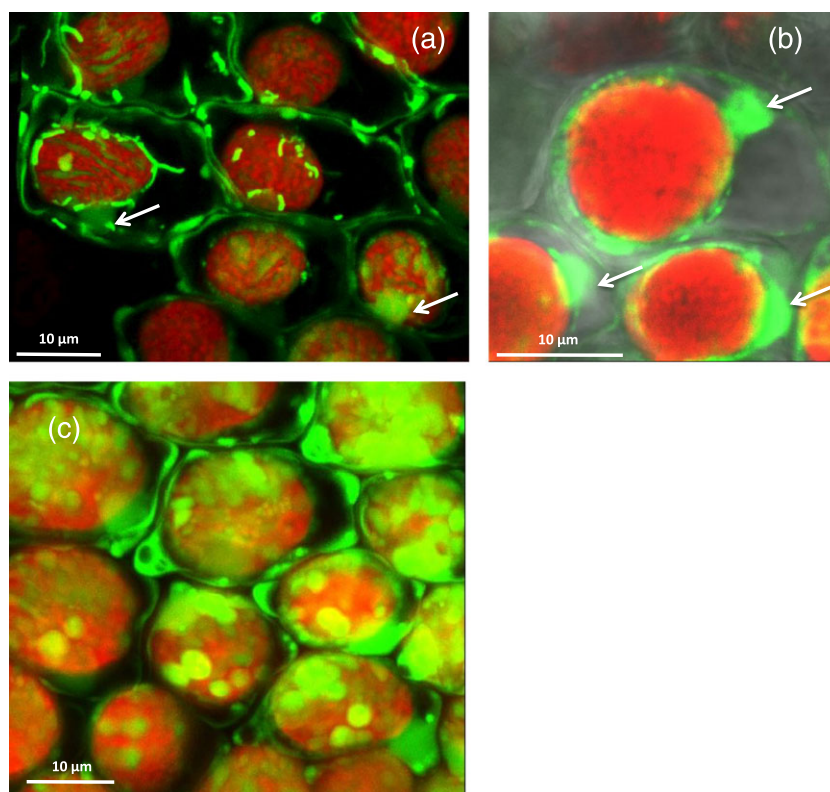


FIGURE 15 Reactive oxygen species in epidermal cells after staining with H2FCDFA dye (in green) in the confocal laser scanning microscopy. Bizonoplasts have red autofluorescence from chlorophyll. (a) Shade adapted control cells: Only some organelles in the cytoplasm including the nucleus (arrows) and the stroma of the bizonoplasts are stained. (b) Illumination with fluorescence light induces a burst of reactive oxygen species from organelles, nucleus, and cytoplasm. (c) Cells treated with high-light intensity had generated a priori high amounts of reactive oxygen species within plastids and the cytoplasm

After exposure of control cells to the microscope illumination for more than 15 s, a tremendous increase of ROS fluorescence is visible throughout the whole cell, emanating from the surroundings of the BZs (Figure 15b). In plants pre-adapted to darkness for 48 hr or more, fluorescence intensity becomes even higher in both the cytoplasm and the BZs.

Treatment with high-light promotes the generation and accumulation of ROS; fluorescence originates from the same organelles as in control plants, but with 120% higher intensity, although in TEM images, no structural alterations can be observed. Moreover, the whole cytoplasm is stained (Figure 15c). If cells are additionally exposed to the microscope illumination, only a slight further increase of fluorescence is triggered.

4 | DISCUSSION

We related structural and physiological reactions of mature giant chloroplasts (BZs) of dark-shade adapted *Selaginella erythropus* to various light conditions mimicking possible situations in the natural environment. In agreement to Sheue et al. (2007, 2015), we found thylakoids in several parallel stacks consisting of three to four thylakoids tightly appressed against each other in the upper zone of BZs extended over the whole plastid surface. The lower zone is differentiated into stroma and grana thylakoids resembling to normal chloroplasts of higher plants (Trissl & Wilhelm, 1993) and some green algae (Gunning & Schwartz, 1999). Detailed inspection of the lower zone in the TEM, however, revealed that almost each thylakoid in the grana stacks is continuous with a thylakoid in the stroma; consequently, thylakoids form uninterrupted extended layers throughout the plastids' lower zone, similar to the thylakoids in the upper zone. In contrast to the upper zone, thylakoids are differentiated into regions of grana stacks where membranes are in tight contact and densely stained by uranyl acetate and lead citrate, and stromal regions where thylakoids are slightly swollen and only faintly stained. The tightly appressed region carrying PSII and LHCII is forming the grana, and non-appressed regions surrounded by plastid stroma carry PSI, LHCI, and ATP synthase complexes (Arvidsson & Sundby, 1999; Heslop-Harrison, 1963; Kirchhoff, Haferkamp, Allen, Epstein, & Mullineaux, 2008).

We were able to link the two zones of BZs to the photosynthetic performance by means of imaging PAM-fluorescence measurements. Whereas the upper zone shows less photosynthetic activity, F_v/F_m is increased in the lower zone containing both grana and stroma thylakoids. The two distinct areas of the BZs are also reflected by changes in fluorescence intensity measured via CLSM: The lower zone has strong fluorescence and appears cup-shaped, but it is not possible to clearly distinguish individual grana. The upper zone has less fluorescence and becomes visible only after careful tuning of the detectors. At around 680 nm, the fluorescence signal is strongest, at 730 nm, a similar fluorescence pattern, but with less intensity becomes apparent. At room temperature, both PSII and PSI show fluorescence (Franck, Juneau, & Popovic, 2002; Pfündel, 1998, 2009) with overlapping emission spectra (Palombi et al., 2011), but so far, the fluorescence signals of PSI and PSII cannot be deconvoluted at the subcellular level. As PSI has a much lower signal contribution to around 10% to the overall fluorescence signal (Pfündel, 2009), the weaker fluorescence emitted from

the upper zone of BZs originates from either PSI and/or low number of PSII. Considering the results obtained from the imaging PAM, and also the ultrastructure from the upper zone of the BZs, we suggest that these thylakoid stacks can be interpreted as very extended grana containing also PSII, but future studies on the supramolecular level are needed to confirm the presence of PSII in this region. The parallel arrangement of thylakoids in the upper zone of BZs reminds of iridoplasts, which occur in dark-shade adapted plants such as the fern *Trichomanes elegans* (Lee, 2007). Iridescence has been discussed as advantageous for efficient light harvesting in *Selaginella* at low-light conditions (Sheue et al., 2007, 2015). Very recently, Jacobs et al. (2016) proved that iridoplasts of *Begonia* increased quantum yield under low-light supply up to 10%. Moreover, absorption of green light was increased. Iridescence, which is caused by optical effects and not pigmentation, is known from various animals and plants (Glover & Whitney, 2010) and it was already studied in the two *Selaginella* species, *S. uncinata* and *S. willdenowii* by Héban and Lee (1984); they found microlayers of epidermal cell walls being responsible for the blue iridescent colour. *S. erythropus* does not show iridescence on a macroscopic level, but this phenomenon could improve irradiance supply and photosynthetic performance within BZs. We moreover assume that crowded stroma thylakoids of the lower zone also increase efficiency of the photosynthetic apparatus.

During prolonged darkness (96 hr), BZs become larger and finally appear darker green than in control plants due to (a) increase in pigment contents (Figure 10), which is linked to (b) higher number of thylakoid stacks in grana. (a) Continued chlorophyll synthesis to enhance size/number of photosynthetic units for a more efficient light absorption was observed in *Tradescantia albiflora* (Kunth) by Adamson, Hiller, and Vesik (1980), who transferred the plant from high-light to 6-day complete darkness. Also, the marine plant *Zostera marina* showed chlorophyll synthesis after transfer to prolonged dark periods of 22 and 47 hr (Adamson, Packer, & Gregory, 1985). Chlorophyll a/b ratio remained similar in *Zostera marina*, which is in accordance to our results. Whereas β -carotene levels per unit biomass remained unchanged irrespective of the treatment, we found a distinct shift of all other major photosynthetic pigments (Figure 10): After 48 hr darkness, a slight decrease was visible followed by a remarkable increase after 96 hr. Based on Chl-a, none of the pigments showed significant changes after 48 hr darkness. From these results, we assume an increase in fresh mass, but no change in pigment content during the first 48 hr darkness. Plants move through a transitory phase, before they start with de novo synthesis of thylakoids via secondary PLBs and pigments after prolonged darkness. (b) The increase of grana discs per stack was already proved in several cases of shade adaption (Kirchhoff et al., 2008). The width of the grana discs, however, only slightly increased in our experiments. This is also in accordance with the suggestions of Kirchhoff et al. (2008) that the diameter of grana stacks has a certain optimal size; it is the same in small and large chloroplasts and responsible for control over dynamic lateral protein diffusion and efficient repair effects.

F_v/F_m of controls and dark-exposed specimens are in the same range (Figure 11), which indicates healthy and intact plants. Prolonged darkness however results in a distinct pattern of RLCs with a slight decrease of ETR_{max} after 48 hr darkness followed by a drop at 96 hr

darkness (Figure 12). Similar responses were also found in diatoms exposed to prolonged darkness (Nymark et al., 2013; Reeves, McMinn, & Martin, 2011). Together with the strong increase in pigment concentrations and the disappearance of PLBs after 96 hr (see below), we assume a transitory phase of *Selaginella*, before substantial changes of the maximum ETR and energy-intense de novo synthesis of pigments will start as a reaction to very low light. From an ecological perspective, this phenomenon can be interpreted as a strategy to cope with prolonged darkness longer than 12 hr, which is a frequent event for small deep-shade plants such as *Selaginella* (e.g., via fallen leaves). If the cover is not removed after a certain prolonged period of darkness between 24 and 48 hr, PLBs formation will start. Between 72 and 96 hr darkness, PLBs are transformed into new thylakoids coinciding with a significant increase of pigments involved in light harvesting.

The de novo formation of PLBs within 48 hr of darkness and their subsequent disappearance have not been observed so far. PLBs have been described during chloroplast biogenesis in darkness. Also, secondary PLBs—so-called recrystallization of PLBs—were described after greening and renewed etiolation in developing leaves (Ikeda, 1970; Lütz, 1981a, 1981b, 1986, 1996; Gunning & Steer, 1996; Solymosi & Schoefs, 2008; Schoefs & Franck, 2008). They were however described in cells undergoing differentiation; they develop as long as the cell is actively synthesizing and forming new thylakoid membranes, that is, before reaching a steady-state situation. In *S. erythropus*, PLBs develop in mature fully differentiated leaves, wherefore we consider them as de novo formation. Their fine structure is quite similar to typical PLBs: They consist of a framework of repeated tubular units that form such regular patterns that they appear crystalline. The organization within the plastid, however, is completely different. While in etioplasts and etio-chloroplasts, one or few large PLBs fill the whole plastid and only few thylakoids emanate from them (Lütz, 1981a, 1981b; Solymosi & Schoefs, 2010), in BZs of *S. erythropus*, the chloroplasts had already developed a mature system of stroma and grana thylakoids; the internal membrane architecture remains intact and to a large extent unaltered. Between grana stacks, stroma thylakoids rearrange and form additional PLBs; emanating tubules connect to stroma and grana thylakoids and interlink grana stacks. Thus, chloroplasts of *S. erythropus* can neither be regarded as etioplasts nor as etio-chloroplasts. In pictures from the literature, we found one similar appearance of chloroplasts, where small PLBs occur within established stroma and grana thylakoid networks (Lütz, 1996); in meristematic cells of the higher plant *Eriophorum angustifolium* differentiating chloroplasts were described after cold treatment, and the importance of temperature in addition to light for chloroplast development was pointed out.

A possible reason for the de novo synthesis of PLBs could be imbalance of the production and accumulation of lipids and ordered arrays of Pchlides (Sperling, Van Cleve, Frick, Apel, & Armstrong, 1997; Sperling et al., 1998; Von Zychlinski et al., 2005; Fong & Archibald, 2008; Blomqvist, Ryberg, & Sundqvist, 2008). Upon illumination, Pchlides would be reduced to chlorophyllides (Schoefs, 2005; Schoefs & Franck, 2003). In darkness, however, Pchlides and enzymes of chlorophyll synthesis accumulate in high density and form PLBs (Minkov, Ryberg, & Sundqvist, 1988; Pyke, 2009; Wrisher, 1973). Various time periods have been reported for the aggregation of Pchlides and appearance of PLBs ranging between 2 days (Hinchman,

1971), 3 days (Lütz, 1981a), and 4 days (Klein & Schiff, 1972; Stetler, 1973). During short periods of darkness such as a natural dark period of one night, this will not become visible, but prolonged absence of light (48 hr in the case of *S. erythropus*) could lead to such significant accumulation of chlorophyll precursors that they aggregate into PLBs.

Another difference between so far described PLBs and the de novo synthesized PLBs of *S. erythropus* is that PLBs of the latter disappear after prolonged darkness, but chlorophyll synthesis continues and grana and stroma thylakoids increase. The ability of some ferns and gymnosperms to produce chlorophyll in the dark has already been established as adaptation to low-light habitats (Adamson et al., 1985; Armstrong, 1998; Hariri & Brangeon, 1977; Lewandowska & Öquist, 1980; Pyke, 2009).

This is to our best knowledge the first time that de novo formation of PLBs in completely differentiated mature chloroplasts was observed. Our results imply that the plasticity of the lamellar system in lower land plants has the potential to overcome prolonged darkness, with secondarily formed PLBs as transition state. The green and healthy appearance of *S. erythropus* during even long dark periods, the regained structure of the chloroplasts after disappearance of PLBs and increased chlorophyll levels as a reaction to lowest light supply underpin this interpretation.

Similar to dark acclimation, BZs increase in size as a first reaction to strong light, but the reason behind is completely different. Major contribution of size originates from an increase of number and size of starch grains; plastids become stuffed with starch grains, which remain and fill almost the whole lower part of BZs, whereas the size of the “green” part gradually decreases with time. These observations are in accordance with other *Selaginella* species (Jagels, 1970b). The increased amount of starch in the BZs under high-light could serve in the first place as energy reservoirs, but it also protects lower grana regions against excess radiation.

Also, the number of grana stacks increases during 48 hr strong light supply; thylakoids of the upper zone are slightly reduced. The characteristic zonation however remains throughout all light treatments indicating a response of the photosynthetic structures to changing light supply, as was suggested already by Shimoni, Rav-Hon, Ohad, Brumfeld, and Reich (2005) and Austin and Staehelin (2011).

The performance of the photosynthetic machinery is continuously adjusted to changing light conditions by the redistribution of light energy between PSI and PSII, that is, stroma and grana thylakoids. Besides changes of the chloroplast micromorphology caused by high-light treatment, also physiological responses were observed. After 48 hr high-light exposure, the decreased F_v/F_m indicate already some damage, which is much more expressed after 96 hr. The lowered pigment amounts explain bleaching of the specimens and together with the lowered F_v/F_m indicate photodamage. Whereas RLCs after 48 hr high-light exposure are still in the range of controls, maximum ETR drops significantly after 96 hr exposure. In contrast to the decrease after prolonged dark periods, we assume that this drop is caused by damage of the photosynthetic apparatus, which is reflected in the microanatomy: whole BZs shrink and retract from the plasma membrane and finally disintegrate into several lobes. The large number of plastoglobuli and the disorientation of the grana stacks remind of the degenerative phase in the chloroplasts' ontogeny called “senescence”

(Biswal, Biswal, & Raval, 2003; Parthier, 1988; Zentgraf, 2007). The lobes remain interconnected by tubules formed from the plastids' envelope. These tubules are filled with stroma and contain no thylakoids and no chlorophyll, hence they are invisible in the fluorescence images. They resemble stromuli that had been described by Holzinger, Buchner, Lütz, and Hanson (2007) and Biswal et al. (2003) for chloroplasts of higher plants. From this stage, chloroplasts never re-greened and microphylls became yellow.

The physiological condition of the chloroplasts was also assessed by measuring ROS formation. ROS serve as second messengers for signalling and trigger defence reactions. When over-produced in high quantity upon various kinds of stress, ROS become toxic (e.g., Fahnenstich, Scarpeci, Valle, Fluegge, & Maurino, 2008; Sharma et al., 2012; Suzuki et al., 2011). BZs from controls and dark treatments have a certain ground level of fluorescence in chloroplasts and other organelles and produce additional ROS mainly upon illumination with the excitation light of the fluorescence microscope. In dark-treated cells, the reaction is more pronounced than in controls; this suggests that the antioxidant system has adapted to light conditions of control plants and scavenges ROS more efficiently than in dark-treated cells. Nevertheless, despite of pre-adaptation, the antioxidant system is also overloaded by microscope light provided suddenly. In cells treated with high-light, the cytoplasm, organelles, and chloroplasts are full of ROS; the detoxifying machinery is not able to remove ROS, and chloroplasts finally decay that is also reflected by the decreased F_v/F_m values (Figures 11, 12, 14) and reduced pigment contents (Figure 10).

5 | CONCLUSIONS

The heterogeneity of BZs is reflected by different activities of PSII with decreased photosynthetic performance in the zone facing the light. We found a de novo formation of PLBs in completely differentiated mature chloroplasts of the mesophyll and BZs after prolonged darkness, which suggests a general response of the plant to impaired light conditions. PLBs disappear after prolonged darkness, which was followed by formation of additional thylakoids. Together with increased contents of LHC-pigments and significantly reduced maximum ETR, plants obviously undergo a transition phase before they start energy-demanding modifications of the photosynthetic apparatus. The green and healthy appearance of *S. erythropus* in long dark periods, high F_v/F_m , and the regained structure of the chloroplasts after disappearance of PLBs underpin this finding. Chloroplasts endure darkness for several weeks in green and functional conditions and increase their photosynthetic apparatus. Immediately after high-light is provided, plants react with increased ROS formation. ROS are an immediate and sensitive indicator for excess light supply, long before the cytoplasm and its organelles show structural damage. Prolonged high-light results in disintegration of chloroplasts and BZs into lobes, which are still connected. Photodamage is reflected by bleaching and significantly decreased F_v/F_m .

ACKNOWLEDGMENTS

We are indebted to our gardeners Andreas Schröfl and Thomas Joch (Dept. Eco genomics & Systems Biology) for taking care of the plants.

This work was funded in parts by Hochschuljubiläumsstiftung der Stadt Wien (H-2115/2010) and Higher Education Commission Pakistan (HEC) to R. Ghaffar.

ORCID

Irene Lichtscheidl  <http://orcid.org/0000-0001-8351-0716>

REFERENCES

- Adamson, H. Y., Hiller, R. G., & Veski, M. (1980). Chloroplast development and the synthesis of chlorophyll a and b and chlorophyll protein complexes I and II in the dark in *Tradescantia albiflora* (Kunth). *Planta*, 150, 269–274.
- Adamson, H. Y., Packer, N., & Gregory, J. (1985). Chloroplast development and the synthesis of chlorophyll and protochlorophyllide in *Zostera* transferred to darkness. *Planta*, 165, 469–476.
- Armstrong, G. A. (1998). Greening in the dark: Light-independent chlorophyll biosynthesis from anoxygenic photosynthetic bacteria to gymnosperms. *Journal of Photochemistry and Photobiology B: Biology*, 43, 87–100.
- Arvidsson, P.-O., & Sundby, C. (1999). A model for the topology of the chloroplast thylakoid membrane. *Australian Journal of Plant Physiology*, 26, 687–694.
- Austin, J. R., & Staehelin, L. A. (2011). Three-dimensional architecture of grana and stroma thylakoids of higher plants as determined by electron tomography. *Plant Physiology*, 155, 1601–1611.
- Biswal, U., Biswal, B., & Raval, M. (2003). *Chloroplast biogenesis*. Dordrecht, The Netherlands: Kluwer Academic.
- Blomqvist, L., Ryberg, M., & Sundqvist, C. (2008). Proteomic analysis of highly purified prolamellar bodies reveals their significance in chloroplast development. *Photosynthesis Research*, 96, 37–50.
- Daims, H., Lückers, S., & Wagner, M. (2006). DAIME, a novel image analysis program for microbial ecology and biofilm research. *Environmental Microbiology*, 8, 200–213.
- Fahnenstich, H., Scarpeci, T. E., Valle, E. M., Fluegge, U.-I., & Maurino, V. G. (2008). Generation of hydrogen peroxide in chloroplasts of *Arabidopsis* overexpressing glycolate as an inducible system to study oxidative stress. *Plant Physiology*, 148, 719–729.
- Fong, A., & Archibald, J. M. (2008). Evolutionary dynamics of light-independent protochlorophyllide oxidoreductase genes in the secondary plastids of cryptophyte algae. *Eukaryotic Cell*, 7(3), 550–553.
- Franck, F., Juneau, P., & Popovic, R. (2002). Resolution of the photosystem I and photosystem II contributions to chlorophyll fluorescence of intact leaves at room temperature. *Biochimica et Biophysica Acta*, 1556, 239–246.
- Glover, B. J., & Whitney, H. M. (2010). Structural colour and iridescence in plants: The poorly studied relations of pigment colour. *Annals of Botany*, 105, 505–511.
- Gunning, B. E. S., & Schwartz, O. M. (1999). Confocal microscopy of thylakoid autofluorescence in relation to origin of grana and phylogeny in the green algae. *Functional Plant Biology*, 26, 695–708.
- Gunning, B. E. S., & Steer, M. (1996). *Plant cell biology: Structure and function*. Inc: Jones and Bartlett Publishers.
- Haberlandt, G. (1888). Die Chlorophyllkörper der Selaginellen. *Flora*, 71, 291–308.
- Haberlandt, G. (1905). Über die Plasmahaut der Chloroplasten in den Assimilationszellen von *Selaginella martensii* Spring. *Berichte der Deutschen Botanischen Gesellschaft*, 23, 441–452.
- Halliwell, B. (2006). Reactive species and antioxidants. Redox biology is a fundamental theme of aerobic life. *Journal of Plant Physiology*, 141, 312–322.
- Hariri, M., & Brangeon, J. (1977). Light-induced adaptive responses under greenhouse and controlled conditions in a fern *Pteris cretica* var.

- ouvrardii I. Structural and infrastructural features. *Physiologia Plantarum*, 41, 280–288.
- Héban, C., & Lee, D. W. (1984). Ultrastructural basis and developmental control of blue iridescence in *Selaginella* leaves. *American Journal of Botany*, 71, 216–219.
- Helfrich, M., Ross, A., King, G. C., Turner, A. G., & Larkum, A. W. (1999). Identification of [8-vinyl]-protochlorophyllide a in phototrophic prokaryotes and algae: Chemical and spectroscopic properties. *Biochimica et Biophysica Acta - Bioenergetics*, 1410, 262–272.
- Heslop-Harrison, J. (1963). Structure and morphogenesis of lamellar systems in grana-containing chloroplasts. I. Membrane structure and lamellar architecture. *Planta*, 60, 243–260.
- Hinchman, R. R. (1971). Early prolamellar body development in oat coleoptile etioplasts. *Annual Report 7870 V. Biochemistry*, 81–82.
- Holzinger, A., Buchner, O., Lütz, C., & Hanson, M. R. (2007). Temperature-sensitive formation of chloroplast protrusions and stromules in mesophyll cells of *Arabidopsis thaliana*. *Protoplasma*, 230, 23–30.
- Iked, T. (1970). Changes in fine structure of prolamellar body in relation to the formation of the chloroplast. *Botanical Magazine Tokyo*, 83, 1–9.
- Jacobs, M., Lopez-Garcia, M., Phrathep, O.-P., Lawson, T., Oulton, R., & Whitney, H. M. (2016). Photonic multilayer structure of *Begonia* chloroplasts enhances photosynthetic efficiency. *Nature Plants*, 2, 16162.
- Jagels, R. (1970a). Photosynthetic apparatus in *Selaginella*. I. Morphology and photosynthesis under different light and temperature regimes. *Canadian Journal of Botany*, 48, 1843–1852.
- Jagels, R. (1970b). Photosynthetic apparatus in *Selaginella*. II. Changes in plastid ultrastructure and pigment content under different light and temperature regimes. *Canadian Journal of Botany*, 48, 1853–1860.
- Jeffrey, S. W., Mantoura, R. F. C., & Wright, S. W. (1997). Phytoplankton pigments in oceanography: Guidelines to modern methods. In *Monographs on oceanographic methodology* (Vol. 10) (p. 661). Paris: UNESCO Publishing.
- Kirchhoff, H., Haferkamp, S., Allen, J. F., Epstein, D., & Mullineaux, C. W. (2008). Significance of macromolecular crowding for protein diffusion in thylakoid membranes of chloroplasts. *Journal of Plant Physiology*, 146, 1571–1578.
- Klein, S., & Schiff, J. A. (1972). The correlated appearance of prolamellar bodies, protochlorophyll(ide) species, and the Shibata shift during the development of bean etioplasts in the dark. *Plant Physiology*, 49, 619–626.
- Lee, D. (2007). Iridescent plants. In D. Lee (Ed.), *Nature's palette. The science of colour* (pp. 262–263). Chicago & London: The University of Chicago Press.
- Lewandowska, M., & Öquist, G. (1980). Structural and functional relationships in developing *Pinus silvestris* chloroplasts. *Physiologia Plantarum*, 48, 39–46.
- Lütz, C. (1981a). Development and ageing of etioplast structures in dark grown leaves of *Avena sativa* (L.). *Protoplasma*, 108, 83–98.
- Lütz, C. (1981b). On the significance of prolamellar bodies in membrane development of etioplasts. *Protoplasma*, 108, 99–115.
- Lütz, C. (1986). Prolamellar bodies. In L. A. Staehelin, & C. J. Arntzen (Eds.), *Encyclopedia of plant physiology* (Vol. 19) (pp. 683–692). Berlin, Heidelberg, New York: Springer.
- Lütz, C. (1996). Avoidance of photoinhibition and examples of photodestruction in high alpine *Eriophorum*. *Journal of Plant Physiology*, 148, 120–128.
- Maxwell, K., & Johnson, G. N. (2000). Chlorophyll fluorescence—A practical guide. *Journal of Experimental Botany*, 51, 659–668.
- Minkov, I. N., Ryberg, M., & Sundqvist, C. (1988). Properties of reformed prolamellar bodies from illuminated and redarkened etiolated wheat plants. *Physiologia Plantarum*, 72, 725–732.
- Mohling Ma, R. (1930). The chloroplasts of *Selaginella*. *Bulletin of the Torrey Botanical Club*, 57, 277–284.
- Nymark, M., Valle, K. C., Hancke, K., Winge, P., Andresen, K., Johnsen, G., ... Brembu, T. (2013). Molecular and photosynthetic responses to prolonged darkness and subsequent acclimation to re-illumination in the Diatom *Phaeodactylum tricornutum*. *PLoS One*, 8, e58722. <https://doi.org/10.1371/journal.pone.0058722>
- Palombi, L., Cecchi, G., Lognoli, D., Raimondi, V., Toci, G., & Agati, G. (2011). A retrieval algorithm to evaluate the photosystem I and photosystem II spectral contributions to leaf chlorophyll fluorescence at physiological temperatures. *Photosynthesis Research*, 108, 225–195.
- Parthier, B. (1988). Gerontoplasts-the yellow end in the ontogenesis of chloroplasts. *Endocytosis. Cell Research*, 5, 163–190.
- Pfündel, E. (1998). Estimating the contribution of photosystem I to total leaf chlorophyll fluorescence. *Photosynthesis Research*, 56, 185–195.
- Pfündel, E. (2009). Deriving room temperature excitation spectra for photosystem I and photosystem II fluorescence in intact leaves from the dependence of FV/FM on excitation wavelength. *Photosynthesis Research*, 100, 163–177.
- Pyke, K. (2009). *Plastid biology*. New York: Cambridge University Press.
- Reeves, S., McMinn, A., & Martin, A. (2011). The effect of prolonged darkness on the growth, recovery and survival of Antarctic sea ice diatoms. *Polar Biology*, 34, 1019–1032.
- Reinbothe, S., Pollmann, S., & Reinbothe, C. (2003). In situ conversion of protochlorophyllide b to protochlorophyllide a in barley. Evidence for a novel role of 7-Formyl reductase in the prolamellar body of etioplasts. *Journal of Biological Chemistry*, 278, 800–806.
- Reshak, A. H., & Sheue, C. R. (2012). Second harmonic generation imaging of the deep shade plant *Selaginella erythropus* using multifunctional two-photon laser scanning microscopy. *Journal of Microscopy*, 248, 234–244.
- Roy, S., Llewellyn, C. A., Egeland, E. S., & Johnsen, G. (2011). *Phytoplankton pigments: Characterization, chemotaxonomy and applications in oceanography*. (p. 845)Cambridge University Press.
- Sarafis, V. (1998). Chloroplast: A structural approach. *Journal of Plant Physiology*, 152, 248–264.
- Schoefs, B. (2005). Protochlorophyllide reduction-what is new in 2005? *Photosynthetica*, 43, 329–343.
- Schoefs, B., & Franck, F. (2003). Protochlorophyllide reduction: Mechanisms and evolution. *Photochemistry and Photobiology*, 78, 543–557.
- Schoefs, B., & Franck, F. (2008). The photoenzymatic cycle of NADPH: protochlorophyllide oxidoreductase in primary bean leaves (*Phaseolus vulgaris*) during the first days of photoperiodic growth. *Photosynthesis Research*, 96, 15–26.
- Schreiber, U., Klughammer, C., & Kolbowski, J. (2012). Assessment of wavelength-dependent parameters of photosynthetic electron transport with a new type of multi-color PAM chlorophyll fluorometer. *Photosynthesis Research*, 113(1–3), 127–144.
- Sharma, P., Jha, A. B., Dubey, R. S., & Pessarakli, M. (2012). Reactive oxygen species, oxidative damage, and antioxidative defense mechanism in plants under stressful conditions. *Journal of Botany*, 2012, 1–27.
- Sheue, C. R., Liu, J. W., Ho, J. F., Yao, A. W., Wu, Y. H., Das, S., & Chesson, P. (2015). A variation on chloroplast development: the bizonoplast and photosynthetic efficiency in the deep-shade plant *Selaginella erythropus*. *American Journal of Botany*, 102, 500–511.
- Sheue, C. R., Sarafis, V., Kiew, R., Liu, H. Y., Salino, A., Kuo-Huang, L. L., ... Ku, M. S. B. (2007). Bizonoplast, a unique chloroplast in the epidermal cells of microphylls in the shade plant *Selaginella erythropus* (Selaginellaceae). *American Journal of Botany*, 94, 1922–1929.
- Shimoni, E., Rav-Hon, O., Ohad, I., Brumfeld, V., & Reich, Z. (2005). Three-dimensional organization of higher-plant chloroplast thylakoid membranes revealed by electron tomography. *The Plant Cell*, 17, 2580–2586.
- Solymosi, K., & Schoefs, B. (2008). Prolamellar body: A unique plastid compartment, which does not only occur in dark-grown leaves. In B.

- Schoefs (Ed.), *Plant cell compartments – Selected topics* (pp. 151–202). Trivandrum: Research Signpost.
- Solymosi, K., & Schoefs, B. (2010). Etioplast and etio-chloroplast formation under natural conditions: The dark side of chlorophyll biosynthesis in angiosperms. *Photosynthesis Research*, 105, 143–166.
- Sperling, U., Franck, F., van Cleve, B., Frick, G., Apel, K., & Armstrong, G. A. (1998). Etioplast differentiation in *Arabidopsis*: Both PORA and PORB restore the prolamellar body and photoactive protochlorophyllide-F655 to the cop1 photomorphogenic mutant. *Plant Cell*, 10, 283–296.
- Sperling, U., Van Cleve, B., Frick, G., Apel, K., & Armstrong, G. A. (1997). Overexpression of light dependent PORA or PORB in plants depleted of endogenous POR by far-red light enhances seedling survival in white light and protects against photooxidative damage. *Plant Journal*, 12, 649–658.
- Stetler, D. A. (1973). Nonphotoconvertible protochlorophyllide in etiolated tissue lacking prolamellar bodies. *Botanical Gazette*, 134, 290–295.
- Suzuki, N., Koussevitzky, S., Mittler, R., & Miller, G. (2011). ROS and redox signalling in the response of plants to abiotic stress. *Plant, Cell and Environment*, 35, 259–270.
- Trissl, H. W., & Wilhelm, C. (1993). Why do thylakoid membranes from higher plants form grana stacks? *Trends in Biochemical Sciences*, 18, 415–419.
- Waterkeyn, L., & Bienfait, A. (1967). Les emergences callosiques et silicifies des feuilles de Selaginelles. *Comptes rendus hebdomadaires des séances de l'Académie des sciences D*, 264, 1608–1611.
- Wright, S. W., Jeffrey, S. W., Mantoura, R. F. C., Llewellyn, C. A., Bjornland, T., Repeta, D., & Welschmeyer, N. (1991). Improved HPLC method for the analysis of chlorophylls and carotenoids from marine phytoplankton. *Marine Ecology Progress Series*, 77, 183–196.
- Wrischer, M. (1973). Ultrastructural changes in isolated plastids II. Etio-chloroplasts. *Protoplasma*, 78, 417–425.
- Zentgraf, U. (2007). Oxidative stress and leaf senescence. In S. Gan (Ed.), *Annual plant review: Senescence processes in plants* (pp. 69–86). Blackwell Publishing Ltd.
- Von Zychlinski, A., Kleffmann, T., Krishnamurthy, N., Sjölander, K., Baginsky, S., & Gruissem, W. (2005). Proteome analysis of the rice etioplast: Metabolic and regulatory networks and novel protein functions. *Molecular & Cellular Proteomics MCP*, 4, 1072–1084.

How to cite this article: Ghaffar R, Weidinger M, Mähner B, Schagerl M, Lichtscheidl I. Adaptive responses of mature giant chloroplasts in the deep-shade lycopod *Selaginella erythropus* to prolonged light and dark periods. *Plant Cell Environ.* 2018;41:1791–1805. <https://doi.org/10.1111/pce.13181>